QUALITY OF MATERIAL DISTRIBUTION IMAGING WITH SEGMENTAL CAPACITIVE SENSOR USING LANDWEBER'S ITERATIVE ALGORITHM

Jakub Lev, Marie Wohlmuthova, Frantisek Kumhala
Czech University of Life Sciences Prague
jlev@tf.czu.cz

Abstract. Yield maps are one of the basic sources of information for practical application of precision agriculture. Yield map creation requires instantaneous yield measurement with adequate quality, best during the harvest. Most of currently used techniques give the information about the amount of material going through the sensor only. Information about the distribution of the material inside of the sensor is not available. The article deals with the segmented capacitive sensor (SCS). The SCS output should be the information about the amount of the material passing through the sensor and also its distribution inside the sensor. The principle of the SCS function is based on multiple measurements of electrical capacity of the air and material mixture. The aim of this paper is to evaluate the possibility of using the Landweber iterative method of image reconstruction for the SCS. Two variants of sensor arrangement were evaluated: with eight electrodes and eight output signals and/or eight electrodes and 56 output signals. A relatively good function of the algorithm was found, however, lower ability to determine the vertical position of the material was also found. For practical use of this type of sensor it is necessary to modify the reconstruction algorithm with the aim of the possibility to include other factors of material behaviour.

Keywords: electrical capacitive tomography, throughput, segmented capacitive sensor.

Introduction

Quality measurement systems for immediate crop yield determination are needed, i.e., for the purpose of yield maps creation. These systems are relatively well sophisticated for the combinable crops. However, this issue is still being addressed, for example, Reinke et al. [1]. On the other hand, throughput measurement in the case of other crops is much less sophisticated. In the case of forage harvesters, a possible cause may be inhomogeneous properties of forage, which are usually harvested. Savoie et al. [2] tested several methods for throughput measurement of material in a forage harvester (torque at the power take-off shaft, at the cutterhead, measuring of the impact energy and capacity controlled oscillator).

Kumhála et al. [3] developed and tested a sensor for the forage throughput measurement in a mowing-conditioning machine. They tested two methods for measuring the throughput of the material: the impact energy measurement and torque of conditioners shaft.

Many methods have been developed for throughput measuring of row crops. For throughput measurement of sugar beet the weighing of harvester working mechanisms are often used [4; 5] Also momentum measure of beet can be used [6]. A sophisticated method was developed by Konstantinovich et al. [7]. They used the wideband radar with which it was possible to determine the number of beet, their location and approximately the yield.

For the measurement of potatoes instantaneous yield similar devices such as for sugar beet are used. A brief overview of these possibilities was published by Algerbo and Ehlert [8]. They described the technologies mainly based on weighing, momentum measuring, radiation methods, and optical methods. An interesting method was tested by Hofstee and Molena [9]. They investigated the instantaneous potato yield measurement based on the machine vision system. When applying this method, impurities of the harvested material caused problems.

For the throughput measurement of agricultural crops it is also possible to use the capacitive method. Kumhala et al. [10] tested the capacitive throughput sensor for potatoes and sugar beet measurement. The capacitive throughput sensor consisted of two plates. The first was connected to the measuring circuit and the other was grounded. The electrical capacity of the air/material mixture was measured. The measurements showed good correlation between the quantity of the material and the level of the electrical capacity. In the same article they also described the theory of the capacitive method. Two methods of filling have been described. Layer filling is characteristic by using the whole plate area for transport of the material through the sensor and the differences in the throughput are realised by increasing the thickness of the analysed material. This regime of the sensor working is typical for materials formed by small particles when the sensor is used for higher throughput values.

Filling by simple particles; in this case the plate area for transport is covered partially and the throughput differences are solved only by the degree of the plate covering that is expressed by the length. This case describes regimes of lower throughputs and/or regimes working with particles which dimensions are nearly comparable with the plates distance. In practical conditions both cases can be combined. Nevertheless, if the average diameter of the measured material particle is relatively small in comparison with the capacitor plate distance the resulting capacity tends to be described as a layer filling depending on the material throughput and conversely, when the average particle dimension is nearly comparable with the plate distance the resulting capacity tends to depend on the throughput as filling by single particle.

Another possibility could be to measure the changes in the capacity from several positions. This principle is used by electrical capacitance tomography (ECT). For example, Williams et al. [11] used the ETC tracking particles on the conveyor. It may very well determine the distribution of particles moving on the conveyor. However, ECT sensors are very complicated and expensive and, moreover, much of the scanning area is unused, since its shape is circular. Slightly better would be the arrangement used by Yang and Liu [12]. It was the ECT sensor consisting of twelve electrodes arranged in a square. Dong and Gou [13] modeled the plane ECT sensor. This sensor would be suitable for the material distributed in a relatively wide layer and could be a suitable alternative for the monitoring of the material moving across the conveyor. Nevertheless, it should be still noted that these sensors are very expensive and their potential for the use in harvesting machines is not too large.

Based on these findings, the idea was to develop a segmented capacitance sensor (SCS), which should be a good compromise between a simple capacitive sensor [10] and ECT sensors. The SCS consists of two main plates that are located one above the other. The lower plate is compact and grounded. The upper plate is divided into segments. During measurement, the material passes between the plates, and the electric capacitance between the segments is measured from the top plate and bottom plate. The main advantage of the SCS is its simplicity. It is accomplished by the measuring of changes in the capacitance in the same ranges (due to a constant distance between the measuring segments and lower ground plates), and so too much smaller demands are addressed to the measuring circuit.

In the ECT and the SCS a suitable reconstruction algorithm is very important. Yang et al. [14] described a reconstruction method based on the Landweber's iterative methods. In another article [15], they conducted a comparison of several known reconstruction algorithms. It has been shown that the method based on Landweber's iteration is relatively accurate and efficient. In this article, Landweber's iterative method was applied to image reconstruction in the SCS. Two cases were compared: measuring sensor with eight segments and eighth output signals and measuring sensor with eighth segments and 56 output signals.

Materials and methods

For the purposes of assessing the quality of image reconstruction, a mathematical model that is shown in Figure 1 was created. To determine the distribution of the electrical potential, the next equation is commonly used:

$$div\left(\varepsilon grad\varphi\right)=0\,, \tag{1}$$

where ε – permittivity, $F\cdot m^{-1}$;
φ – electrical scalar potential, V.

The mathematical model of the SCS is shown in Figure 1. It consists of two copper plates. The top plate was divided into eight segments. In the first option, the number of the output signals was eight. Voltage was connected to one of the segments ($\varphi = 1$) and the electric capacity of the mixture of air and material between the bottom plate and segment was measured. The lower plate was grounded ($\varphi = 0$ V). Other segments were completely disconnected from the electrical potential. Since it is known that the presence of a conductive material affects the electric potential distribution, these properties must be taken into account. In this article, disconnected electrodes have been described as an area with very high relative permittivity ($\varepsilon_r = 10^6$) [16].

In the second option, one segment was connected with the source of voltage (φ = 1), while one of the remaining seven, was connected with half of this voltage (φ = 0.5 V). In this way it was obtained 8 × 7, it means 56 signals.

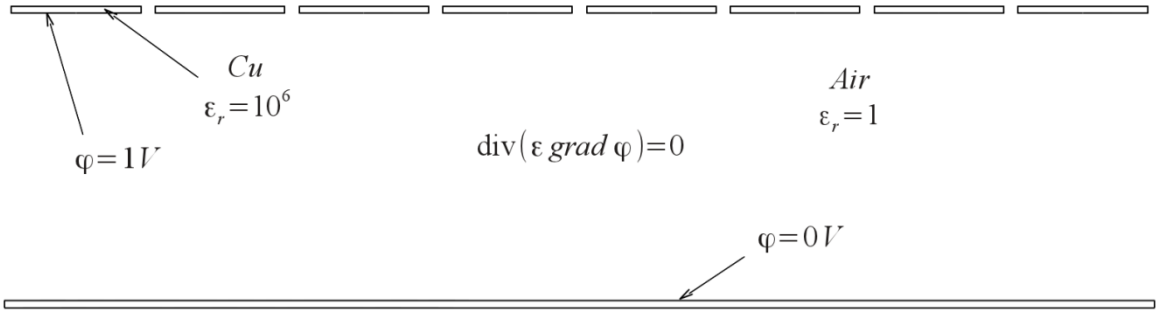

Fig. 1. **Mathematical model of the segmented capacitance sensor (SCS)**

In both cases, equation 1 was solved by the finite element method using hp-adaptive algorithms with the help of Agros2D software. The capacity was then calculated from the total energy of the electric field. The following equation was used:

$$C = \frac{2E}{U^2} \tag{2}$$

where C – electrical capacity, F;
E – energy of electric field, J;
U – voltage between electrodes, V.

When solving the inverse problem, the next matrix equation is expected [14]:

$$C = S \cdot G \tag{3}$$

where C – $m \times 1$ vector of capacitance changes;
G – $n \times 1$ vector of permittivity distribution;
S – $m \times n$ matrix of sensitivity maps.

The matrix of sensitivity maps was determined on the base of the equations published by Xie et al. [17]:

$$S_i(k) = \frac{C_i(k) - C_{iair}}{C_{imaterial} - C_{iair}}, \tag{4}$$

where S_i – sensitivity map for connection of electrodes i;
i – variant connection of electrodes (i = 1, 2, ..., 8 or 1, 2, ..., 56);
k – k-th pixel in sensitivity map (k = 1, 2, ..., 64 or 1, 2, ..., 256);
$C_i(k)$ – electrical capacity for connection of electrodes i and k-th pixel;
C_{iair} – electrical capacity for empty sensor and connection of electrodes i;
$C_{imaterial}$ – electrical capacity for full sensor and connection of electrodes i.

The dimensions of the sensing area of the sensor were 200 mm in height and 800 mm in width. The scanning segments were 80 mm wide. The gap between the adjacent segments was 20 mm. The plate thickness was 1 mm. Computing resolutions for the first option 4 × 16 and the second option 8 × 32 were chosen.

For deriving the vector G from equation 3 it was necessary to obtain the matrix S^{-1}. This was problematic because the matrix S has a rectangular shape. When we name $\overline{G}$ as the estimated permittivity distribution, then it can be written:

$$\overline{G} = S^T \cdot C \tag{5}$$

According to Yang et al. [14] the Landweber's iteration method for accurate determination of $\overline{G}$ can be taken. The authors used the following formula:

$$\overline{G_{k+1}} = \overline{G_k} + \alpha \cdot S^T \left(C - S \cdot \overline{G_k} \right), \tag{6}$$

where α – gain factor.

The initial $\bar{G}_0$ vector is chosen as zero. For more enhancements it is possible to modify the equation 6:

$$\overline{G_{k+1}} = f\left[\overline{G_k} + \alpha \cdot S^T \left(C - S \cdot \overline{G_k} \right) \right], \tag{7}$$

where f – a nonlinear function, which regulates the elements:

$$f(x) = \begin{cases} 0, & x < 0 \\ f(x), & 0 \le x \le 1 \\ 1, & x > 1 \end{cases} \tag{8}$$

For α it is possible to apply the following criterion:

$$\left\| \alpha \cdot S^T \cdot S \right\|_2 < 2 \tag{9}$$

In this paper, α was chosen to be in the first option $\alpha = 900$ and in the second option $\alpha = 490$. Both values meet the convergence criteria of the equation 9.

For purposes of evaluating the applicability of the reconstruction algorithm, three variants of the tested material distribution were used: a) triangle, b) continuous layer of material, and c) two rectangular objects in the middle of the sensor. The iteration was described by equation 7 and it was programmed in the Scilab 5.3 computer software. 500 iterations were chosen.

Results and discussion

The results of this solution can be seen in Figure 2. The first column shows the test distribution of permittivity, the second column (option 1) shows a variant with eight output signals and a resolution of 4 × 16, and the third column (option 2) shows a variant with 56 output signals and a resolution of 8 × 32.

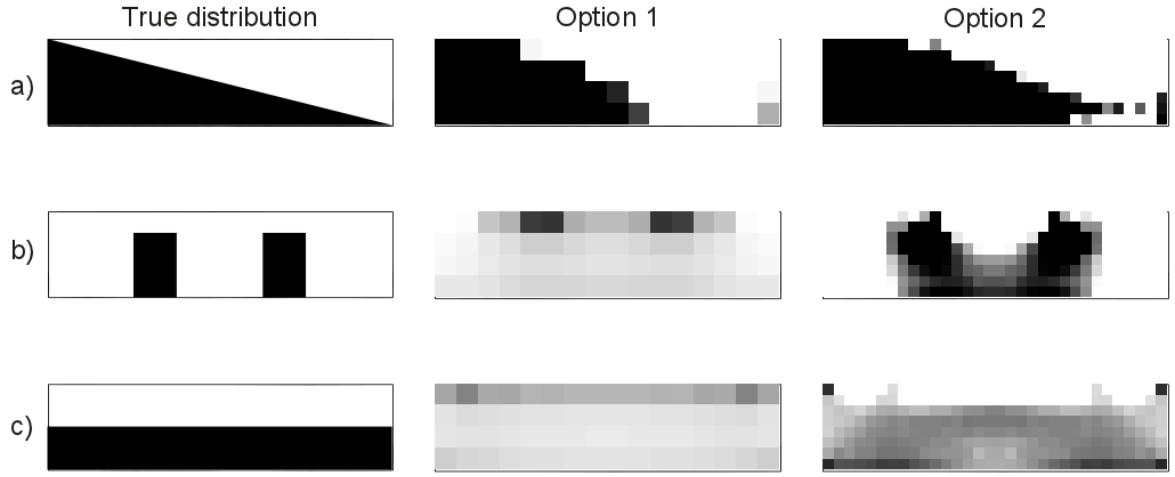

Fig. 2. **Images reconstructed from simulated data**

The first test permittivity distribution in the shape of a triangle can be reconstructed relatively well. Good pictures can be seen in both options 1 and 2. In order to compare the two variants the relative error and the correlation coefficient were calculated. The following formulas were used for calculation:

$$RE = \frac{\left\| \hat{g} - g \right\|}{\left\| g \right\|} \tag{10}$$

$$CC = \frac{\sum_{i=1}^{N}\left(\hat{g}_i - \overline{\hat{g}}\right)\left(g_i - \overline{g}\right)}{\sqrt{\sum_{i=1}^{N}\left(\hat{g}_i - \overline{\hat{g}}\right)^2\left(g_i - \overline{g}\right)^2}} \tag{11}$$

where RE – relative image error;
$\hat{g}$ – vector of reconstructed permittivity distribution;
g – vector of true permittivity distribution;
$\overline{\hat{g}}$ – mean values of $\hat{g}$;
$\overline{g}$ – mean values of g.

For option 1 it was counted: RE = 44.3 % and CC = 0.803. For option 2 it was counted: RE = 45.9 % and CC = 0.793. It is evident from both, the image and from the calculated values, that the results are almost identical for both variants. Even according to the calculated parameters, it seems that better results are provided by the first option.

The second example test shows the permittivity distribution for two rectangular objects in the middle of the sensor. It is immediately apparent from Figure 2 that the results of the reconstruction were not satisfied. As a result using option 1, the two rectangles were reduced to four pixels from the top of the sensor only. In option 2, although the picture seems subjectively more similar to the original, big differences still exist. The third test example (continuous layer) also shows a low quality result. As in the first and the second option there has been some scattered distribution of permittivity for the greater part of the scanned area. In both cases it was decided that the differences are so high that it makes no sense to count the relative error and the correlation coefficients of the image.

An interesting finding may be similar errors in option 1 with the distribution of permittivity testing b and c. Two major errors can be observed in both cases. The distribution of material is shown at the top of the sensor (not at the bottom where it should be) and its area is reduced relatively considerably. These two errors are linked together, of course; as it is evident from the mathematical model shown in Figure 1, the electric potential gradient near the electrodes is higher than in other places, it means that the sensitivity in these places is much higher. So, logically the same response produces a smaller amount of material.

In Option 2 it can be observed that a larger number of output signals bring slightly better results. In both cases it is possible to estimate that the true position of the material is rather at the bottom of the sensor than in the top. The question remains whether by seven time greater number of measurements a reasonable efficiency is achieved. Dubious can also be a sufficient independence of each measurement, regardless of the fact that this measurement may be technically complicated.

Conclusions

Three simulations with three different test permittivity distributions were performed for the purposes of evaluating the applicability of the reconstruction algorithm based on the Landweber's iterative methods for the SCS sensor. Based on the simulations, it can be stated that relatively good results were achieved during the test with triangle distribution of permittivity. Nevertheless, certain errors were also found. Particularly evident was the error in material vertical detection. There is an effort from the algorithm to place the material into the top of the sensor. In option 2, this error rate is reduced; however, it is clear that the improvement does not increase in accordance with increased number of the measurements. It is likely that the measurements are not sufficiently independent.

Based on these findings, it is possible to derive that the reconstruction algorithm based on the Landweber's iterative method is not suitable for the SCS. Likely, the main reason will be in low numbers of possible independent measurements. For the function of the SCS it is therefore necessary to look for other possibilities of evaluation of the measured capacitance changes and add other factors and assumptions of material behavior to the mathematical model. The effects of the Earth's gravity can be a useful example.

References

1. Reinke R., Dankowicz H., Phelan J., Kang W. A dynamic grain flow model for a mass flow yield sensor on a combine. Precision Agriculture, 2011. In print. DOI 10.1007/s11119-010-9215-0
2. Savoie P., Lemire P., Theriault R. Evaluation of five sensors to estimate mass-flow rate and moisture of grass in a forage harvester. Applied Engineering in Agriculture, 2002. 18, 389–397.
3. Kumhála F., Kroulík M., Prošek V. Development and evaluation of forage yield measure sensors in a mowing-conditioning machine. Computers and Electronics in Agriculture,2007. 58, 2, p. 154 - 163. ISSN: 0168-1699.
4. Walter J. D., Backer L. F.Sugarbeet Yield Monitoring for Site-Specific Farming Part I-Laboratory Tests and Preliminary Field Tests. Precision Agriculture, 4, 2003 (4), p. 421-431.
5. Hall T. L., Backer L. F., Hofman V. L.Sugarbeet Yield Monito-ring for Site-Specific Farming Part II-Field Testing. Precision Agriculture, 4, 2003 (4), p. 433-444.
6. HennensD.,Baert J.,Broos B., Ramon H., Baerdemaeker J. De. Development of a Flow Model for the Design of a Momentum Type Beet Flow Sensor. Biosystems Engineering, 85, 2003 (4), p. 425-436.
7. Konstantinovic M.,Woeckel S., Schulze Lammers P., Sachs J. Evaluation of a UWB Radar System for Yield Mapping of Sugar Beet. ASABE Paper No. 071051, ASA-BE, St. Joseph, Michigan, 2007, 12 p.
8. Ehlert D., Algerbo P.-A. 2000. Yielding mapping with potatoes. Landtechnik, 55, 2000: 436–437.
9. Hofstee J W., Molena GJ. Machine vision based yield mapping of potatoes. 2002. ASAE Paper No. 021200, 10 p.
10. Kumhála F., Prošek V., Blahovec J. Capacitive throughput sensor for sugar beets and potatoes. Biosystems Engineering. 2009. 102, 36-43.
11. Williams R. A., Luke S. P., Ostrowski K. L., Bennett M. A. Measurement of bulk particulates on belt conveyor using dielectric tomography. Chemical Engineering Journal. 2000. 77, 57-63.
12. Yang W. Q., Liu S. Electrical capacitive tomography with a square sensor. In: Proceedings of the 1st World Congress on Industrial Processes Tomography, 14-17 April 1999, pp. 313-317, Buxton, UK.
13. Dong X., Guo S.Modelling planar array sensor for electrical capacitance tomography. In: Proceedings of Second International Conference on Modelling and Simulation, 21-22 May 2009, 5 p., Manchester, UK.
14. Yang W. Q., Spink D. M., York T. A., McCann H. An image-reconstruction algorithm based on Landweber's iteration method for electrical-capacitance tomography. Meas. Sci Technol. 10 (1999) 1065-1069.Printed in the UK
15. Yang W. Q., Peng L. Image reconstruction algorithms for electrical capacitance tomography. Meas. Sci. Technol. 14 (2003) R1-R13.
16. Konrad A., Graovac M. The Finite Modeling of Conductors and Floating Potentials. IEEE Transactions on magnetics. Vol. 32. No. 5. September 1996.
    XieC. G., Huang S. M., Hoyle B. S., Thorn R.,Lenn C. Snowden D. Beck M. S. Electrical capacitance tomography for flow imaging: system model for the development of image reconstruction algorithms and design of primary sensors. IEE Proceedings-G 139 (1992) 89-98.
17. Scilab. [online] [10.3.2012]. Available et: http://www.scilab.org/support/documentation.
18. Agros2D. [online] [10.3.2012]. Available et:http://agros2d.org.